J. Biochem. 129, 411–421 (2001)

Purification and Characterization of Homo- and Hetero-Dimeric Acetate Kinases from the Sulfate-Reducing Bacterium *Desulfovibrio vulgaris*[1]

Ling Yu,* Tetsuo Ishida,*,[2] Kiyoshi Ozawa,† Hideo Akutsu,† and Kihachiro Horiike*

Department of Biochemistry, Shiga University of Medical Science, Seta, Ohtsu, Shiga 520-2192; and †Department of Bioengineering, Faculty of Engineering, Yokohama National University, 156 Tokiwadai, Hodogaya-ku, Yokohama 240-8501

Received November 10, 2000; accepted December 15, 2000

Two distinct forms of acetate kinase were purified to homogeneity from a sulfate-reducing bacterium *Desulfovibrio vulgaris* Miyazaki F. The enzymes were separated from the soluble fraction of the cells on anion exchange columns. One acetate kinase (AK-I) was a homodimer ($\alpha^S{}_2$) and the other (AK-II) was a heterodimer ($\alpha^S\alpha^L$). On SDS-PAGE, α^L and α^S subunits migrated as bands of 49.3 and 47.8 kDa, respectively, but they had an identical N-terminal amino acid sequence. A rapid HPLC method was developed to directly measure ADP and ATP in assay mixtures. Initial velocity data for AK-I and AK-II were collected by this method and analyzed based on a random sequential mechanism, assuming rapid equilibrium for the substrate binding steps. All kinetic parameters for both the forward acetyl phosphate formation and the reverse ATP formation catalyzed by AK-I and AK-II were successfully determined. The two enzymes showed similar kinetic properties in Mg^{2+} requirement, pH-dependence and magnitude of kinetic parameters. These results suggest that two forms of acetate kinase are produced to finely regulate the enzyme function by post-translational modifications of a primary gene product in *Desulfovibrio vulgaris*.

Key words: acetate kinase, HPLC analyses of ADP and ATP, kinetics, post-translational modification, sulfate-reducing bacterium.

Sulfate-reducing bacteria are widespread in nature and play important roles in the sulfur cycles in soil, sediments from freshwater and marine environments, and deep-sea hydrothermal vents (*1–3*). In wastewater treatment facilities, sulfate-reducing bacteria enhance corrosion of the facilities in concert with sulfide-oxidizing bacteria in wastewater biofilms (*4*, *5*). New sulfate reducers belonging to the genus *Desulfovibrio* have been isolated recently from roots of seagrass (*6*), and the intestine of humans and animals (*7*). A strain isolated from estuarine sediments can carry out reductive dehalogenation (*8*). A new biosynthetic pathway of porphyrins has been found in *Desulfovibrio vulgaris* (*9*, *10*). These recent advances in the studies of the sulfate-reducing bacteria have raised many questions about their physiology and biochemistry.

Acetate kinase (ATP:acetate phosphotransferase, EC 2.7.2.1) catalyzes the following reaction.

$$\text{acetate} + \text{ATP} \rightleftharpoons \text{acetyl phosphate} + \text{ADP} \quad (1)$$

The forward reaction is important for microbes to activate acetate when acetate is the sole carbon source available (*11*) and when acetyl phosphate is produced to regulate microbial functions such as flagellar expression (*12*, *13*). By the reverse reaction, most facultative and strictly anaerobic microbes can obtain ATP by substrate-level phosphorylation.

Figure 1 summarizes bioenergetics of sulfate reduction in the genus *Desulfovibrio* when the bacteria grow on lactate and sulfate (*14*). On the one hand, the bacteria generate two ATPs by phosphorylation at the substrate level coupled to the oxidation of two molecules of pyruvate. On the other hand, one ATP is consumed to activate sulfate to adenosine-5′-phosphosulfate and another ATP is used to regenerate two ADPs. Net production of ATP cannot be attained only by substrate-level phosphorylation. For growth on lactate and sulfate, therefore, *Desulfovibrio* has an obligatory requirement for electron-transfer coupled phosphorylation for net production of ATP. Despite the importance of the reaction catalyzed by acetate kinase in energy metabolism in *Desulfovibrio*, there has been no report on acetate kinase in sulfate-reducing bacteria since the early work done by Brown and Akagi (*15*) on the enzyme in *Desulfovibrio desulfuricans*.

In recent years, molecular cloning of the acetate kinase gene has been done for various microbes to understand the physiological roles of the enzyme and sometimes to address the mechanism of enzymatic phosphoryl transfer reaction (*16–19*). Acetate kinases have also been purified from *Bacillus stearothermophilus* (*20*), *Veillonella alcalescens* (*21*, *22*),

[1] This work was supported in part by Grants-in-Aid for Scientific Research from the Ministry of Education, Science, Sports and Culture of Japan.

[2] To whom correspondence should be addressed. Fax: +81-77-548-2157, Phone: +81-77-548-2158, E-mail: teishida@belle.shiga-med.ac.jp

Abbreviation: AK, acetate kinase.

2 lactate → 2 pyruvate + 4 e + 4 H^+	(lactate dehydrogenase)
2 pyruvate + 2 CoA → 2 acetyl-CoA + 2 CO_2 + 4e + 2H^+	(pyruvate:ferredoxin oxidoreductase)
2 acetyl-CoA + 2 Pi → 2 acetyl phosphate + 2 CoA	(phosphotransacetylase)
2 acetyl phosphate + 2 ADP → 2 acetate + 2 ATP	(acetate kinase)
SO_4^{2-} + ATP → APS + PPi	(ATP sulfurylase)
PPi + H_2O → 2 Pi	(inorganic pyrophosphatase)
APS + 2 e → SO_3^{2-} + AMP	(APS reductase)
AMP + ATP → 2 ADP	(adenylate kinase)
SO_3^{2-} + 6 e + 8 H^+ → H_2S + 3 H_2O	(sulfite reductase)
2 lactate + SO_4^{2-} + 2 H^+ → 2 acetate + 2 CO_2 + H_2S + 2 H_2O	net reaction

Fig. 1. **Bioenergetics of *D. vulgaris* cells growing on lactate and sulfate.** The bioenergetics of sulfate reduction in *Desulfovibrio* reported by Liu and Deck (*14*) is summarized in this figure with modifications. No net formation of ATP occurs at the substrate level. Three molecules of ATP are formed in an electron-transfer-coupled manner during the reduction of one molecule of sulfite to sulfide. APS, adenosine-5′-phosphosulfate; PP_i, inorganic pyrophosphate; P_i, inorganic phosphate.

Acholeplasma laidlawii (*23*), Spirochete MA-2 (*24*), *Salmonella typhimurium* (*25*), *Escherichia coli* (*25*), *Methanosarcina thermophila* (*26*), *Clostridum acetobutylicum* (*27, 28*), and *Thermotoga maritima* (*29*). Acetate kinase from all these microbes is a homodimer except the enzyme from *B. stearothermophilus*, which is a homotetramer. These enzymes show mainly similar kinetic properties but substantial differences such aspects as enzyme stability, susceptibility to sulfhydryl reagents, sensitivity to succinate or fructose 1,6-bisphosphate, and magnitude of kinetic parameters. Recent progress in X-ray crystallographic study on acetate kinase from *M. thermophila* (Archaea domain) (*30*) has stimulated reexamination of the mechanism of phosphoryl transfer and new studies on the structural basis of difference in kinetic properties among acetate kinases.

In this study, we purified two forms of acetate kinase from *Desulfovibrio vulgaris* Miyazaki F cells by separation on an anion-exchange column. One was a homodimer, the other a heterodimer. The presence of two acetate kinases has been reported only for an anaerobic marine spirochete (spirochete MA-2) (*24*), and a heterodimeric acetate kinase has never been reported. To examine the kinetic properties of the purified enzymes in detail, we developed a HPLC method to measure directly nucleotides (ADP or ATP) formed in assay mixtures. We did not use the conventional enzyme-coupled methods for kinetic experiments of acetate kinase (*20–29*) because addition of hexokinase, glucose-6-phosphate dehydrogenase, pyruvate kinase, lactate dehydrogenase, and their substrates make reaction mixtures too complex and therefore vulnerable to systematic experimental errors. In the present direct assay of products, reaction mixtures contained simply substrates for acetate kinase and a catalytic amount of the enzyme. We applied a random sequential model to the initial velocity data obtained by the present methods and successfully determined all kinetic parameters contained in the model.

MATERIALS AND METHODS

Materials—*D. vulgaris* Miyazaki F was cultured anaerobically on a Postgate medium C (*31*). The bacterial cells were collected by centrifuging the culture medium, and the cell pellets were kept at −80°C until use. ATP disodium salt, GTP sodium salt, and acetyl phosphate lithium potassium salt were purchased from Sigma. ADP disodium salt and FAD were purchased from Nacalai Tesque. All other chemicals were of reagent grade.

Purification of Acetate Kinase—D. vulgaris Miyazaki F cells (39.0 g) were homogenized in 100 ml of 20 mM Tris-HCl (pH 7.7) containing 2 mM DTT and 1 mM EDTA (buffer A) by sonication. DNase I (Sigma, 2 mg) was added to the homogenate. After 10 min of incubation in ice-water, the homogenate was centrifuged at 16,000 ×*g* for 30 min at 4°C. The supernatant (crude extract) was diluted to 390 ml with buffer A and then applied to a DEAE-Toyopearl column (5 × 14 cm, Tosoh) preequilibrated with the buffer. The column was washed with 600 ml of buffer A, then developed with a linear gradient of 0–0.12 M NaCl in a total volume of 1.4 liters of the same buffer. The column was further washed with 500 ml of buffer A containing 0.12 M NaCl. Acetate kinase activities eluted as two adjacent but well-separated peaks (see Fig. 2A). The enzyme activities contained in the first peak (fractions 93–96) and the second peak (fractions 100–106) were pooled separately and designated as AK-I and AK-II, respectively.

Both AK-I and AK-II fractions (DEAE-Toyopearl) were further purified by the same procedures. In the following, we describe the purification of AK-I. The DEAE-Toyopearl fraction was 3-fold diluted with cold 10 mM Tris-HCl (pH 7.3) and applied to a Q-Sepharose column (2.5 × 22.0 cm, Pharmacia) preequilibrated with 50 mM Tris-HCl (pH 7.3) containing 2 mM DTT. The enzyme was eluted with a linear concentration gradient of 0–0.2 M NaCl in 1 liter of the equilibration buffer. The active fractions (Q-Sepharose) were collected and concentrated to 0.46 ml by ultrafiltration with a Centriflo CF25 membrane cone (Amicon) and a Microcon YM-30 membrane filter (Amicon).

The concentrated Q-Separose fraction was further purified by gel-filtration on a TSKgel G3000SW_{XL} column (7.8 × 300 mm, Tosoh). Aliquots (20 μl) of the concentrate were repeatedly injected into the column preequilibrated with 50 mM Tris-HCl (pH 7.3) containing 0.3 M NaCl and 2 mM DTT. Elution was performed with the same buffer at a flow rate of 0.3 ml/min. The pooled active fractions (TSKgel G3000SW_{XL}) were concentrated to about 0.4 ml by ultrafiltration with a Microcon YM-30 membrane filter. The concentrated sample was 5-fold diluted with 20 mM Tris-HCl (pH 7.4) and injected into a Mono Q HR5/5 column preequilibrated with 50 mM Tris-HCl (pH 7.4) containing 2 mM DTT. The column was developed with a linear gradient of NaCl concentration (7.5 mM/min) in the equilibration buffer. The flow rate of 0.5 ml/min. The active fractions (Mono Q) were pooled and concentrated to about 0.1 ml by ultrafiltration with a Microcon YM-10 membrane filter.

Aliquots (20 μl) of the concentrated Mono Q fraction were repeatedly injected into a TSKgel SuperSW3000 col-

umn (4.6 × 300 mm, Tosoh) preequilibrated with 50 mM Tris-HCl (pH 7.3) containing 0.3 M NaCl and 2 mM DTT. Elution was performed with the same buffer at a flow rate of 0.2 ml/min. The fractions with high activity and least contamination as judged by SDS-PAGE were pooled (TSKgel SuperSW3000).

Assay for Acetate Kinase Activity—At each purification step the hydroxamate assay (*32*) was used to assay acetate kinase activity. The formation of acetyl phosphate from acetate and ATP was detected by this method. The reaction mixture (0.20 ml) contained 50 mM Tris-HCl (pH 8.3), 50 mM succinate, 5 mM ATP, 5 mM $MgCl_2$, 50 mM sodium acetate, 0.5 M NH_2OH, and an enzyme solution. The reaction was started by the addition of 10 μl of 1 M sodium acetate, allowed to proceed at 37°C for 10–20 min, and stopped by the addition of 0.3 ml of $FeCl_3$-trichloroacetic acid solution (0.37 M $FeCl_3$, 0.2 M trichloroacetic acid, 0.68 M HCl). The absorbance at 540 nm due to the hydroxamate-ferric ion complex was measured with a Multiscan microplate reader (Labsystems). For reagent control and calibration, aqueous solutions containing various known amounts of acetyl phosphate were added to the reaction mixtures instead of enzyme solutions.

Initial velocity in the forward reaction was determined for purified enzymes by direct measurement of ADP formation. All kinetic assays were performed at 25°C. The assay mixture (0.1 ml) contained 50 mM HEPES (pH 7.5), 50 mM NaCl, 5 mM $MgCl_2$, sodium acetate (0–0.1 M), ATP (0–5 mM) and enzyme solution. The reaction mixture without acetate was preincubated for 5 min at 25°C, and the reaction was started by the addition of 10 μl of acetate solution. The mixture was incubated at 25°C for 5–20 min, then the reaction was stopped by the addition of 0.1 ml of 0.5 M potassium phosphate (pH 3.0), and 10 μl of 0.5 mM FAD was added as an internal standard. An aliquot (5 μl) of the final mixture was injected into a Mono Q HR5/5 column, and FAD and ADP were rapidly separated by the elution with 20% acetonitrile and 80% 0.26 M potassium phosphate (pH 3.0) (v/v). The flow rate was 1.0 ml/min, and elution of FAD and ADP was detected by monitoring absorbance at 260 nm. The unreacted ATP that bound tightly to the column was washed out with 20% acetonitrile and 80% 0.5 M potassium phosphate (pH 3.0) (v/v), and the column was reequilibrated with the elution buffer before injection of the next sample. It took 12 min in total to analyze one sample. A CCPM-II pump, an AS-8021 automatic sample injector equipped with a sample holder kept at 4°C, a Chromatocorder 21 integrator, all from Tosoh, and a Shimadzu SPD-10Avp UV-VIS detector were used for automatic HPLC analyses.

Initial velocity in the reverse reaction was determined by direct measurement of ATP formation. The assay mixture (0.1 ml) contained 50 mM HEPES (pH 7.5), 50 mM NaCl, 10 mM $MgCl_2$, acetyl phosphate (0–5 mM), ADP (0–10 mM), and enzyme solutions. The reaction mixture without acetyl phosphate was preincubated for 5 min at 25°C, and the reaction was started by the addition of 10 μl of acetyl phosphate solution. The mixture was incubated at 25°C for 5–20 min. The reaction was stopped by the addition of 0.1 ml of 1.0 M potassium phosphate (pH 3.0), and 20 μl of 1 mM GTP was added as an internal standard. An aliquot (5 μl) of the final mixture was injected into a Mono Q HR5/5 column, and ATP and GTP were rapidly separated by the elution with 20% acetonitrile and 80% 0.42 M potassium phosphate (pH 3.0) (v/v). The flow rate was 1.0 ml/min, and absorbance at 260 nm was monitored.

SDS–polyacrylamide Gel Electrophoresis—SDS-PAGE was performed on a 10% gel according to Laemmli (*33*) under the reducing conditions. Aliquots (2.0 μl) of samples were mixed with 7.5 μl of Laemmli's sample buffer, incubated at 80°C for 3 min, and electrophoresed on a 10% SDS-PAGE gel. Proteins were stained with Coomassie Brilliant Blue by using a staining kit (Wako Pure Chemical Industries).

To determine the NH_2-terminal amino acid sequences of the acetate kinases, aliquots (1 μg, 14–24 μl) of purified AK-I and AK-II were electrophoresed in a 10% SDS-PAGE gel after treatment with 7.5 μl of Laemmli's sample buffer. The separated proteins were electro-transferred to a PVDF membrane (Clear Blot Membrane-P, ATTO) with a semi-dry blotter (AE-6677-S, ATTO) and stained with Coomassie Brilliant Blue. The membrane was rinsed three times with 50% methanol. The protein bands at 47.8 and 49.3 kDa were excised and each of the membrane slices was directly subjected to an Applied Biosystems 477A sequencer and a 120A PTH analyzer. The marker proteins were purchased from Boehringer Mannheim.

Molecular Weight Determination—The molecular weight of native acetate kinase was determined by low-angle laser light scattering measurement combined with gel chromatography (*34*, *35*). A TSKgel G3000SW_{XL} column (7.8 × 300 mm), an LS-8000 low-angle laser light scattering photometer, both from Tosoh, and a Shimadzu RID-6A differential refractometer were used. The buffer was 50 mM Tris-HCl (pH 7.4) containing 0.3 M NaCl and the flow rate was 0.4 ml/min. The molecular weight standards used were bovine ribonuclease-A (M_r = 13,700), bovine albumin monomer (M_r = 66,300) and tetrameric catechol 2,3-dioxygenase (*Pseudomonas putida*, M_r = 140,624); the former two proteins were from Sigma and the third was purified by the reported method (*36*).

The subunit molecular weight of acetate kinase was determined by matrix-assisted laser desorption mass spectrometry. The purified enzymes (10 μl each) were desalted by HPLC on a Cosmosil 5C4 AR300 column (2.0 × 150 mm). The desalted enzymes were mixed with α-cyano-4-hydroxycinnamic acid (a matrix-forming material). Mass spectra were obtained on a Voyager-DE RP mass spectrometer (PerSeptive Biosystems). Catechol 2,3-dioxygenase (35,156 Da) and bovine serum albumin (66,300 Da) were used for mass calibration.

Other Analytical Methods—Protein concentrations of crude samples were measured in a final reaction volume of 420 μl with a dye reagent (Bio-Rad), and those of purified enzyme were estimated in a final reaction volume of 120 μl with the dye reagent by using a Shimadzu UV-2200 spectrophotometer equipped with an ultramicro cell holder. Bovine γ-globulin was used as a standard protein. The concentrations of the purified enzymes determined by the dye reagent were converted to the respective molar subunit concentrations by using the subunit molecular weight of 44,270, which was determined by mass spectrometry described above.

Kinetic Models—Blätter and Knowles (*37*) have clearly demonstrated that acetate kinase reaction proceeds with net steric inversion on the transferring phosphorus atom.

This fact is most simply explained by a direct in-line transfer of phosphoryl from donor to acceptor in a ternary enzyme-donor-acceptor complex (*37*, *38*). Initial velocity data are therefore expected to obey either a random sequential Bi Bi mechanism or an ordered sequential Bi Bi mechanism (*39*). Another important finding, that a specific glutamate residue is phosphorylated when acetate kinase is incubated with acetyl phosphate or ATP alone, has raised controversy about whether the acyl-phosphate form is an obligatory covalent intermediate in the catalysis. The catalytic mechanism of acetate kinase is still poorly understood. To date, relatively thorough kinetic studies of acetate kinase have been done only for the enzyme from *Escherichia coli* (*40*, *42–44*) and a large discrepancy is found among the reported results for *E. coli* acetate kinase.

In this study, kinetic data for the forward reaction (acetyl phosphate formation) and the reverse reaction (ATP formation) were analyzed based on a random mechanism in which all steps for substrate binding are in rapid equilibrium. Then, the forward and reverse reactions are expressed by the following Eqs. 2 and 3, respectively.

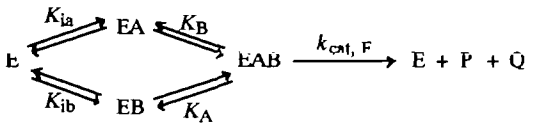

(2)

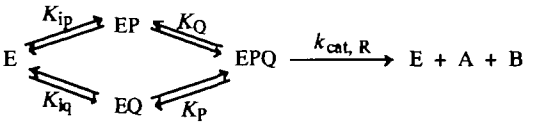

(3)

where A, B, P, and Q are acetate, ATP, acetyl phosphate, and ADP, respectively. The kinetic constants (K_{ia}, K_A, K_{ib}, K_B, K_{ip}, K_P, K_{iq}, and K_Q) are dissociation constants for the respective binding reactions.

In these models, initial velocities (v_F and v_R) are given as follows.

$$v_F = \frac{k_{cat,F}E_tAB}{K_{ia}K_B + K_BA + K_AB + AB} \quad (4)$$

$$v_R = \frac{k_{cat,R}E_tPQ}{K_{ip}K_Q + K_QP + K_PQ + PQ} \quad (5)$$

where E_t is the total subunit concentration of acetate kinase and italic letters are the concentrations of the corresponding substrates. The following relations exist among the equilibrium constants.

$$K_{ib} = \frac{K_{ia}K_B}{K_A} \quad (6)$$

$$K_{ip} = \frac{K_{iq}K_P}{K_Q} \quad (7)$$

Rate equations for an ordered sequential Bi Bi mechanism are given by the same equations as Eqs. 4 and 5, although the kinetic parameters have different meanings from those in the rapid equilibrium random mechanism explained above. To differentiate random and ordered sequential mechanisms, inhibition of the forward reaction by acetyl phosphate was examined.

Data Processing—All kinetic data obtained in the present study fitted well to a simple hyperbolic curve. We first determined apparent V_{max} and K_m values by s/v *versus* s plots, where v is the initial velocity and s is substrate concentration. Then, the theoretical v *versus* s curve was drawn using the V_{max} and K_m values obtained above, and the data were plotted on the curve. The goodness of the fit was easily confirmed by inspection of the deviation of the data points from the theoretical hyperbola.

From Eq. 4, the apparent V_{max} (V_A^{app}) and K_m (K_A^{app}) for acetate under the ATP concentration of B are expressed as follows.

$$V_A^{app} = k_{cat,F}E_t\left(\frac{B}{K_B + B}\right) \quad (8)$$

$$K_A^{app} = K_A + \frac{(K_{ia} - K_A)K_B}{(K_B + B)} \quad (9)$$

From Eqs. 5 and 7, the apparent V_{max} (V_Q^{app}) and K_m (K_Q^{app}) for ADP under the acetyl phosphate concentration of P are expressed as follows.

$$V_Q^{app} = k_{cat,R}E_t\left(\frac{P}{K_P + P}\right) \quad (10)$$

$$K_Q^{app} = K_Q + \frac{(K_{iq} - K_Q)K_P}{(K_P + P)} \quad (11)$$

The values of $k_{cat,F}$ and K_B were first obtained from B/V_A^{app} *versus* B plots on the basis of Eq. 8 and then those of K_A and K_{ia} were obtained from K_A^{app} *versus* $\frac{K_B}{(K_B+B)}$ plots on the basis of Eq. 9. The value of K_{ib} was finally obtained by using Eq. 6. All kinetic parameters for the reverse reaction (Eq. 3) could be determined in the same way as for the forward reaction in using Eqs. 7, 10, and 11.

RESULTS

Purification of Acetate Kinases—From the soluble fraction of *D. vulgaris* Miyazaki F cells, two acetate kinase activities were separated almost completely by anion-exchange chromatography on a DEAE-Toyopearl column using a gradient of increasing NaCl concentration (Fig. 2A).

The enzyme eluted first (fractions 93–96 in Fig. 2A) and that eluted just after the first enzyme (fractions 100–106 in Fig. 2A) were collected separately and designated as acetate kinase–I (AK-I) and acetate kinase–II (AK-II), respectively. The total activity of AK-I was about 1.8-fold higher than that of AK-II. AK-I and AK-II were further purified by anion-exchange chromatography on a Q-Sepharose column and then by gel filtration on a TSKgel G3000SW$_{XL}$ column (chromatograms not shown).

The partially purified AK-I and AK-II obtained in the three chromatographic purification steps described above were then subjected to a Mono Q column (Fig. 2, B and C, respectively). AK-II showed slightly higher affinity to the column than AK-I, consistent with the chromatographic behavior on the first anion-exchange chromatography on a DEAE-Toyopearl column (Fig. 2A). A small amount of AK-II contaminating the partially purified AK-I was separated as a shoulder to the main peak by this chromatography (Fig. 2B).

Figure 2, D and E, shows SDS-PAGE analyses of the AK-I and AK-II fractions with high acetate kinase activities, respectively. The AK-I fractions contained one dominant protein band (47.8 kDa) and two weak ones (57.4 and 76.4

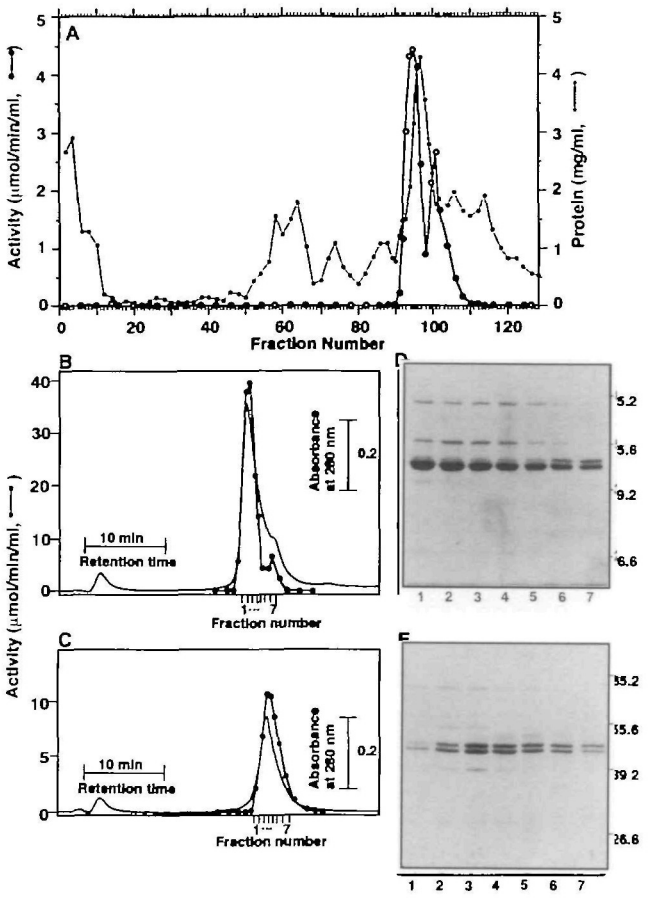

Fig. 2. **Chromatographic separation of two acetate kinase activities from *D. vulgaris* Miyazaki F cells.** A: The crude extract prepared from 39 g of the bacterial cells was applied to a DEAE-Toyopearl column (5.0 × 14.0 cm) preequilibrated with 20 mM Tris-HCl (pH 7.7) containing 2 mM DTT and 1 mM EDTA as described under "MATERIALS AND METHODS." The bound proteins were first eluted with a linear gradient of 0–0.12 M NaCl concentration built in 1.4 liters of the buffer and then with 500 ml of the buffer containing 0.12 M NaCl. Acetate kinase activity was measured by the hydroxamate method as described under "MATERIALS AND METHODS" using 50 mM sodium acetate and 5 mM ATP (with 5 mM $MgCl_2$) as substrates. The active fractions eluted as the first peak and those eluted as the second peak just after the first peak were separately collected and designated as AK-I and AK-II, respectively. B: The AK-I active fractions obtained by gel filtration on a TSKgel G3000SW_{XL} (the third purification step) were applied to a Mono Q HR5/5 column preequilibrated with 50 mM Tris-HCl (pH 7.4) containing 2 mM DTT as described under "MATERIALS AND METHODS." The column was developed at the flow rate of 0.5 ml/min with a linear gradient of NaCl concentration (7.5 mM/min) in the equilibration buffer. C: The AK-II active fractions obtained by gel filtration on a TSKgel G3000SW_{XL} were subjected to a Mono Q HR5/5 column by the same procedures as for AK-I. D: Aliquots (2.5 μl each) of the AK-I Mono Q fractions with a high activity (the fractions 1–7 in the Fig. 2B) were 5-fold diluted with distilled water, incubated with 10 μl of SDS buffer containing 2-mercaptoethanol at 80°C for 3 min, and then analyzed by SDS-PAGE on a 10% gel. The proteins were stained with Coomasssie Brilliant Blue. The lane number corresponds to the respective number of Mono Q fractions applied to the lane. The positions of the molecular weight markers and the respective molecular mass (kDa) are shown on the right side. E: The AK-II Mono Q fractions with a high activity (the fractions 1–7 in the Fig. 2C) were analyzed by SDS-PAGE as described above for the AK-I fractions.

kDa), while the AK-II fractions showed two major bands (47.8 and 49.3 kDa) with an equal amount of proteins.

The Mono Q fractions (fractions 1–4 for AK-I and 2–6 for AK-II) were combined and subjected to gel filtration on a TSKgel SuperSW3000 column, the final purification step. Both enzymes were eluted as a single peak at the same elution volume (data not shown). Tables I and II summarize the purification of AK-I and AK-II, respectively.

AK-I was finally purified 110-fold (28.3 μmol/min/mg) with a yield of 2.0%, while AK-II was purified 76-fold (19.6 μmol/min/mg) with a yield of 0.5%. The respective yields indicate that both AK-I and AK-II represent about 1% of the soluble *D. vulgaris* protein. Purified AK-I and AK-II could be stored in 50 mM Tris-HCl (pH 7.4) containing 0.3 M NaCl and 2 mM DTT at −20°C for several months without loss of activity.

Molecular Characterization of AK-I and AK-II—As shown in Fig. 3A, SDS-PAGE revealed the presence of only one subunit with apparent molecular mass of 47.8 kDa for AK-I, but two subunits with apparent molecular mass of 47.8 and 49.3 kDa for AK-II. The N-terminal amino acid sequences of the AK-I subunit (47.8 kDa) and the two AK-II subunits (47.8- and 49.3-kDa subunits) were determined. All subunits had an identical sequence of MNVLVINSGSSSIKYQLIDMTTEKAL, strongly suggesting that the AK-I subunit and the 47.8 kDa AK-II subunit are same protein, and that the two AK-II subunits are products of a single gene. We designate the 47.8- and 49.3-kDa subunits as α^S and α^L subunits, respectively. The N-terminal amino acid sequence of the acetate kinase shows high identity with those in organisms belonging to the Bacteria or Archaea domains, especially 86% identity to that in *Methanosarcina thermophila* (*30*). The N-terminus of acetate kinases is suggested to bind nucleotide-β-phosphate, because the sequence is similar to the consensus sequence for the nucleotide-β-phosphate loop in the sugar kinase/hsp70/actin superfamily.

The purified AK-I and AK-II were subjected to mass spectrometry after desalting by HPLC on a small Cosmosil 5C4 column. Only one molecular peak with molecular mass of 44,270 Da was detected for both purified enzymes (data not shown), contrasting to the results obtained by SDS-PAGE. The molecular weight of native AK-I and AK-II was determined to be 8.35×10^4 and 8.48×10^4, respectively, by low-angle laser light scattering photometry coupled with high-performance gel chromatography (Fig. 3B). These results indicate a homodimer ($\alpha^S{}_2$) structure for AK-I and a heterodimer ($\alpha^S\alpha^L$) structure for AK-II.

Kinetic Characterization of AK-I and AK-II—Initial velocity in the forward reaction was measured as a function of acetate concentration for purified AK-I and AK-II by direct measurement of ADP formation, rather than the enzyme-coupled assay commonly used for kinetic experiments of acetate kinase. Figure 4A shows a linear relation between the ratio of ADP and FAD peak areas (inset, Fig. 4A) and the ADP concentration in the reaction mixtures. The good linear relation was obtained for a wide ADP concentration range of 10–500 μM.

Figure 4B shows the dependence of initial velocity of AK-I as measured by the rate of ADP formation on the acetate concentration under the fixed ATP concentration of 3.0 mM. The *v versus s* data fitted well to a simple hyperbolic curve, and the apparent V_{max} and K_m values obtained were

64.3 μM/min and 27.9 mM, respectively. In the presence of the fixed ATP concentrations of 0.25, 0.5, 1.0, 3.0, and 5.0 mM, the dependence of initial velocity of AK-I and AK-II on the acetate concentration was examined (Fig. 5, A and C, respectively).

On the basis of Eqs. 8 and 9, the apparent V_{max} (V_A^{app}) and K_m (K_A^{app}) values for acetate as functions of ATP concentration were analyzed. Figure 6A shows V_A^{app} *versus* B plots for AK-I and AK-II (B is the ATP concentration). Both data for AK-I and AK-II fitted well to a hyperbolic curve, and the $k_{cat,F}E_t$ and K_B values for AK-I obtained were 99.0 μM/min and 2.15 mM, respectively; the $k_{cat,F}E_t$ and K_B values for AK-II were 96.9 μM/min and 3.40 mM, respectively. By using the respective total enzyme concentration (E_t) of 4.56 and 5.22 nM, the turnover number for the forward reaction ($k_{cat,F}$) for AK-I and AK-II was calculated to be 362 and 310 s^{-1}, respectively.

The K_A^{app} values were plotted against $K_B/(K_B+B)$ values, which were calculated with the obtained K_B value (Fig. 6C). Both K_A^{app} *versus* $K_B/(K_B+B)$ data for AK-I and AK-II fitted fairly well to linear relation of Eq. 9. The intercept on K_A^{app}–axis gave the K_A values for AK-I and AK-II of 30.6 and 26.9 mM, respectively. The slope gave the $K_{ia}-K_A$ value, and by adding the K_A value to the slope we obtained K_{ia} value. Finally, by using Eq. 6 the K_{ib} value was obtained. The results are summarized in Table III.

Initial velocity in the reverse reaction was measured as a function of ADP concentration for purified AK-I and AK-II by direct measurement of ATP formation. Figure 4C shows a linear relation between the ratio of ATP and GTP peak areas (inset, Fig. 4C) and the ATP concentration in the reaction mixtures. In the presence of 10 mM ADP, the calibration line did not pass through the origin but intercepted the (ATP)/(GTP)–axis at 1.32, indicating that the commercial ADP used contained ATP as a contaminant at the level of 2%. Despite the substantial levels of contaminating ATP in the ADP preparation, a good linear relation was obtained for a wide ATP concentration range of 10–500 μM. This enabled us to discriminate enzymatically formed ATP from the contaminating ATP.

Figure 4D shows the dependence of initial velocity of AK-I as measured by the rate of ATP formation on the ADP concentration under the fixed acetyl phosphate concentration of 2.5 mM. The v *versus* s data fitted well to a simple hyperbolic curve, and the apparent V_{max} and K_m values for ADP obtained were 125 μM/min and 1.12 mM, respectively. In the presence of fixed acetyl phosphate concentrations of 0.5, 1.0, 2.5, and 5.0 mM, the dependence of initial velocity of AK-I and AK-II on the ADP concentration was examined (Fig. 5, B and D, respectively). On the basis of Eqs. 7, 10 and 11, the $V_A^{app'}$ and $K_A^{app'}$ data as functions of ATP concentration were analyzed as described above for the forward reaction (Fig. 6, B and D). The kinetic parameters obtained are summarized in Table IV.

Inhibition of the forward reaction by acetyl phosphate was examined (Fig. 7). Acetyl phosphate showed competitive inhibition against both substrates, acetate (Fig. 7, A

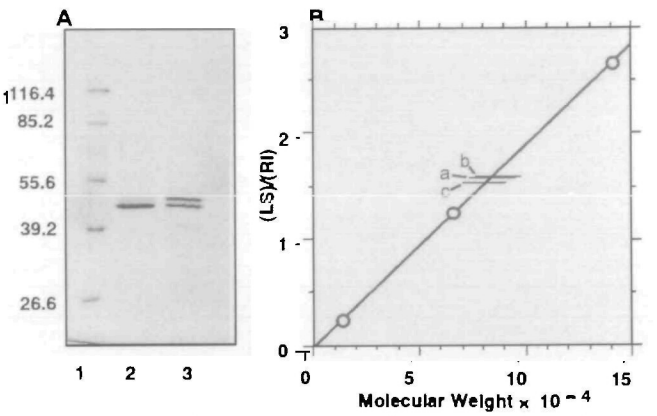

Fig. 3. **Molecular Characterization of AK-I and AK-II.** A: Aliquots of 1 μg of the finally purified AK-I (lane 2) and AK-II (lane 3) were subjected to SDS-PAGE on a 10% gel. The proteins were stained with Coomasssie Brilliant Blue. Lane 1 shows the marker proteins and the values on the left side are the respective molecular mass expressed in kDa. B: Aliquots (10 μl) of the finally purified AK-I (a), AK-II (b), and a mixture of the two enzymes (c) were each subjected to gel filtration on a TSKgel G3000SW$_{XL}$ column (7.8 × 300 mm) and the components in the eluates were detected by a low-angle laser light scattering photometer and a differential refractmeter in this order. The elution buffer was 50 mM Tris-HCl (pH 7.4), 0.3 M NaCl, and the flow rate was 0.4 ml/min. The ratio of the output of the light scattering photometer (LS) to that of the refractmeter (RI) was plotted against molecular weight.

TABLE I. **Purification of acetate kinase I in the soluble fraction of the *Desulfovibrio vulgaris* cells.**

Purification step	Total Volume (ml)	Total activity (μmol/min)	Total protein (mg)	Specific activity (μmol/min/mg)	Purification (fold)	Yield (%)
Crude extract	116	1,252	4,860	0.258	1	100
DEAE-Toyopearl	76.0	399	227	1.76	6.82	31.9
Q-Sepharose	71.9	238	36.4	6.54	25.3	19.0
TSKgel G3000SW$_{XL}$	4.7	115	6.72	17.1	66.3	9.2
Mono Q	1.9	47.1	2.55	18.5	71.7	3.8
TSKgel SuperSW3000	0.78	25.2	0.89	28.3	110	2.0

TABLE II. **Purification of acetate kinase II in the soluble fraction of the *Desulfovibrio vulgaris* cells.**

Purification step	Total Volume (ml)	Total activity (μmol/min)	Total protein (mg)	Specific activity (μmol/min/mg)	Purification (fold)	Yield (%)
Crude extract	116	1,252	4,860	0.258	1	100
DEAE-Toyopearl	136	226	234	0.966	3.74	18.1
Q-Sepharose	53.6	71.8	18.7	3.84	14.9	5.7
TSKgel G3000SW$_{XL}$	1.9	25.7	2.01	12.8	49.6	2.1
Mono Q	1.57	13.5	0.81	16.7	64.7	1.1
TSKgel SuperSW3000	0.27	6.36	0.32	19.6	76.0	0.51

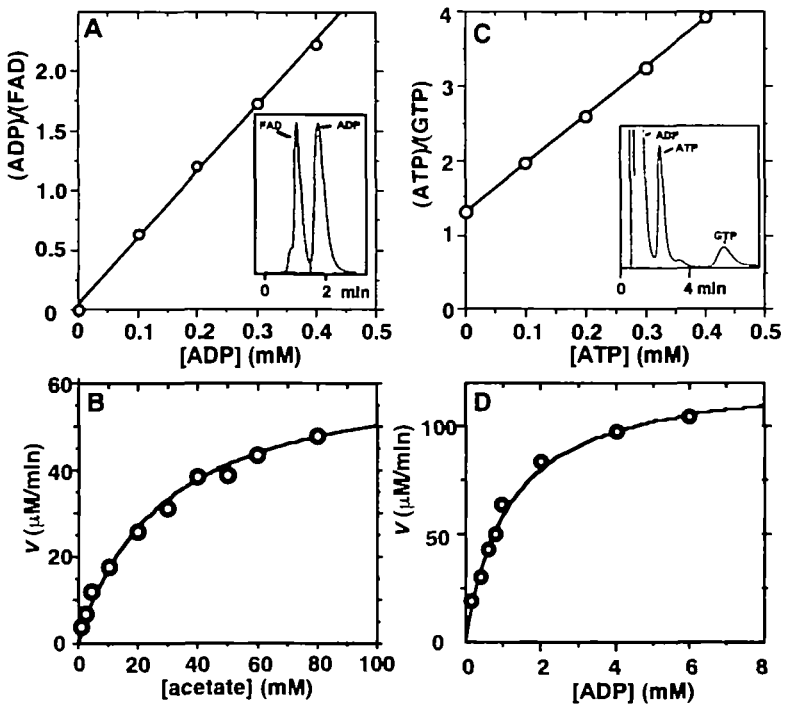

Fig. 4. **Kinetic analyses of the forward and reverse reactions by measuring ADP and ATP.** A: Reaction mixtures (0.1 ml) containing 5.0 mM ATP, 5.0 mM $MgCl_2$, 50 mM HEPES (pH 7.5), 50 mM NaCl, and the indicated concentrations of ADP were prepared. The mixtures were incubated at 25°C for 11 min, then an equal volume of 0.5 M potassium phosphate (pH 3.0) and 5 nmol FAD (10 μl of 0.5 mM FAD) was added to each mixtures. After vigorous mixing, an aliquot (5 μl) of each sample was injected into a Mono Q HR5/5 column preequilibrated with acetonitrile/0.26 M potassium phosphate (pH 3.0) = 20/80 (v/v). The column was developed with the same solvent at a flow rate of 1.0 ml/min and absorbance at 260 nm was monitored. Inset shows a typical chromatogram obtained with the sample containing 0.2 mM ADP. The ratio of the peak areas of ADP (ADP), and FAD (FAD) was plotted against the ADP concentration. B: Initial velocities were measured for the forward reaction catalyzed by AK-I (E_t = 4.65 nM) at 25°C in 50 mM HEPES (pH 7.5) and plotted against acetate concentrations in the reaction mixtures. The reaction mixtures contained 3.0 mM ATP, 5.0 mM $MgCl_2$, and the indicated concentrations of acetate. After the reaction was stopped and an aliquot of the sample subjected to HPLC as described above, the amount of ADP was determined by using the linear relation between the (ADP)/(FAD) ratio and ADP concentrations obtained above. The theoretical curve in the figure was drawn with apparent V_{max} and K_m values of 64.3 μM/min and 27.9 mM, respectively. C: Reaction mixtures (0.1 ml) containing 10.0 mM ADP, 10.0 mM $MgCl_2$, 50 mM HEPES (pH 7.5), 50 mM NaCl, and the indicated concentrations of ATP were prepared. The mixtures were incubated at 25°C for 9.0 min, then an equal volume of 1.0 M potassium phosphate (pH 3.0) and 20 nmol GTP (20 μl of 1 mM GTP) was added to each mixture. After vigorous vortexing, an aliquot (5 μl) of each sample was injected into a Mono Q HR5/5 column preequilibrated with acetonitrile/0.42 M potassium phosphate (pH 3.0) = 20/80 (v/v). The column was developed with the same solvent at a flow rate of 1.0 ml/min and absorbance at 260 nm was monitored. Inset shows a typical chromatogram obtained with the sample containing 0.1 mM ATP. The ratio of the peak areas of ATP (ATP) and GTP (GTP) was plotted against the ATP concentration. D: Initial velocities were measured for the backward reaction catalyzed by AK-I (E_t = 4.65 nM) at 25°C in 50 mM HEPES (pH 7.5) and plotted against ADP concentrations in the reaction mixtures. The reaction mixtures contained 2.5 mM acetyl phosphate, 10.0 mM $MgCl_2$, and the indicated concentrations of ADP. After the reaction was stopped and an aliquot of the sample subjected to HPLC as described above, the amount of ATP was determined by using the linear relation between the ATP/GTP peak ratio and ATP concentrations obtained above. The theoretical curve in the figure was drawn with apparent V_{max} and K_m values of 125 μM/min and 1.12 mM, respectively.

and C) and ATP (Fig. 7, B and D). The results suggested that both enzyme reactions follow a rapid equilibrium random sequential mechanism.

Effect of Mg^{2+} Concentration on Acetate Kinase Reaction—Figure 8 shows the data for the Mg^{2+} ion dependence for the forward reaction catalyzed by AK-I and AK-II. When Mg^{2+} ion was absent, neither acetate kinase showed measurable activity. The activities of AK-I and AK-II increased almost linearly as Mg^{2+} concentration increased from 0 to 5 mM ($[Mg^{2+}]/[ATP]$ = 1.0), while a further increase in Mg^{2+} concentration up to 10 mM ($[Mg^{2+}]/[ATP]$ = 2.0) did not change their activities. These results confirmed that acetate kinase requires a Mg^{2+}-nucleotide complex as substrate, and that a moderate excess of Mg^{2+} does not inhibit the activity of AK-I or AK-II. In the kinetic experiments done in the present study, we used HEPES as a buffer, which has a low metal-complexing capacity, and the concentrations of Mg^{2+} in assay mixtures were always higher than those of ATP or ADP.

Effect of pH on Acetate Kinase Reaction—The pH optimum of the acetate kinase reaction was measured in the direction of acetyl phosphate synthesis (Fig. 9). Both AK-I and AK-II showed a high activity (70–100% of the maximum activity) over a broad pH range of 7.0–8.5, and the shapes of the respective pH curves for AK-I and AK-II were generally similar. The pH curve of AK-I showed a plateau in the pH region of 7.0–8.5, and that of AK-II showed a near plateau in the same pH region where AK-II activity slightly increased with the increase in pH value from 7.0 to 8.5.

In the present study, the acetate kinase reaction was terminated by the addition of an equal volume of 0.5–1.0 M potassium phosphate (pH 3.0) to the reaction mixture. After this treatment, the pH values of the samples were less than 5.0, usually in the range of 4.0–5.0, as directly determined by a pH meter. Neither enzyme showed measurable activity at pH range lower than 5.0, supporting the effectiveness of the present method to stop the enzymatic reaction.

DISCUSSION

In this study, two forms of acetate kinase were for the first time purified to homogeneity from *Desulfovibrio vulgaris* Miyazaki F. The two enzymes were separated on an anion-exchange column, like the two isoenzymes from a spirochete (*24*). One enzyme (AK-I) was a homodimer and the other (AK-II) was a heterodimer. They shared one common

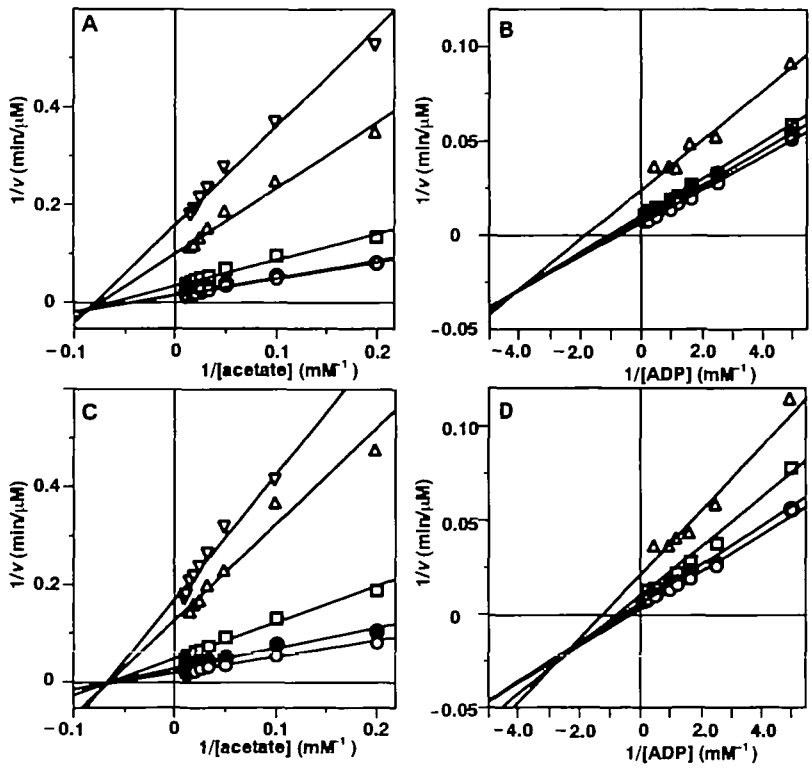

Fig. 5. **Initial velocity pattern for AK-I and AK-II with acetate (in the forward reaction) and ADP (in the reverse reaction) as the varied substrates.** A: Initial velocities were measured for the forward reaction catalyzed by AK-I (E_t = 4.56 nM) under the fixed ATP concentrations of 0.25 (▽), 0.5 (△), 1.0 (□), 3.0 (●), and 5.0 (○) mM. B: Initial velocities were measured for the reverse reaction catalyzed by AK-I (E_t = 4.56 nM) under the fixed acetyl phosphate concentrations of 0.5 (△), 1.0 (□), 2.5 (●), and 5.0 (○) mM. C: Initial velocities were measured for the forward reaction catalyzed by AK-II (E_t = 5.22 nM) under the fixed ATP concentrations D: Initial velocities were measured for the reverse reaction catalyzed by AK-II (E_t = 10.3 nM) under the fixed acetyl phosphate concentrations.

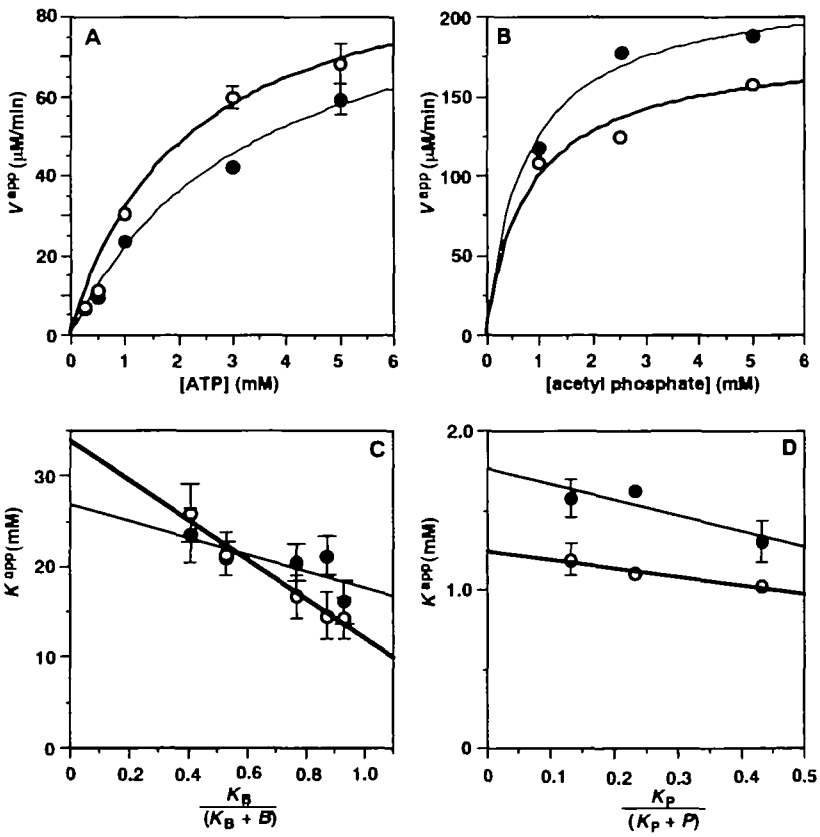

Fig. 6. **Analyses of apparent V_{max} and K_m for acetate as functions of ATP concentration (in the forward reaction) and those for ADP as functions of acetyl phosphate (in the reverse reaction).** The apparent V_{max} and K_m values for acetate were obtained for the fixed ATP concentrations of 0.25, 0.5, 1.0, 3.0, and 5.0 mM. The apparent V_{max} and K_m values for ADP were obtained for the fixed acetyl phosphate concentrations of 1.0, 2.5, and 5.0 mM. Open circles, AK-I; closed circles, AK-II. The error bars show standard deviation (SD). Data points without error bars means that SD values are less than the radius of the open or closed circles used. A: The apparent V_{max} was plotted against ATP concentration. The theoretical curves in the figure were drawn on the basis of Eq. 8 with the $k_{cat,P}E_t$ and K_B values of 99.0 μM/min and 2.15 mM for AK-I, and with those values of 96.9 μM/min and 3.40 mM for AK-II. B: The apparent V_{max} was plotted against acetyl phosphate concentration. The theoretical curves in the figure were drawn on the basis of Eq. 10 with the $k_{cat,R}E_t$ and K_p values of 180 μM/min and 0.834 mM for AK-I, and 219 μM/min and 0.758 mM for AK-II. C: The apparent K_m value was plotted against $K_B/(K_B+B)$, where B is the ATP concentration and K_B value of 2.15 mM for AK-I and 3.40 mM for AK-II. K_m versus $K_B/(K_B+B)$ data were analyzed on the basis of Eq. 9. D: The apparent K_m value was plotted against $K_p/(K_p+P)$, where P is the acetyl phosphate concentration and K_p value of 0.834 mM for AK-I and 0.758 mM for AK-II. K_m versus $K_p/(K_p+P)$ data were analyzed on the basis of Eq. 11.

subunit (α^S), and the subunit unique to AK-II (α^L) had an identical N-terminal amino acid sequence to the α^S subunit. α^S Subunit migrated at an apparent molecular mass of 47.8 kDa, while α^L subunit migrated at that of 49.3 kDa. Both enzymes, however, showed only one molecular peak with similar molecular mass. These results suggest that α^L sub-

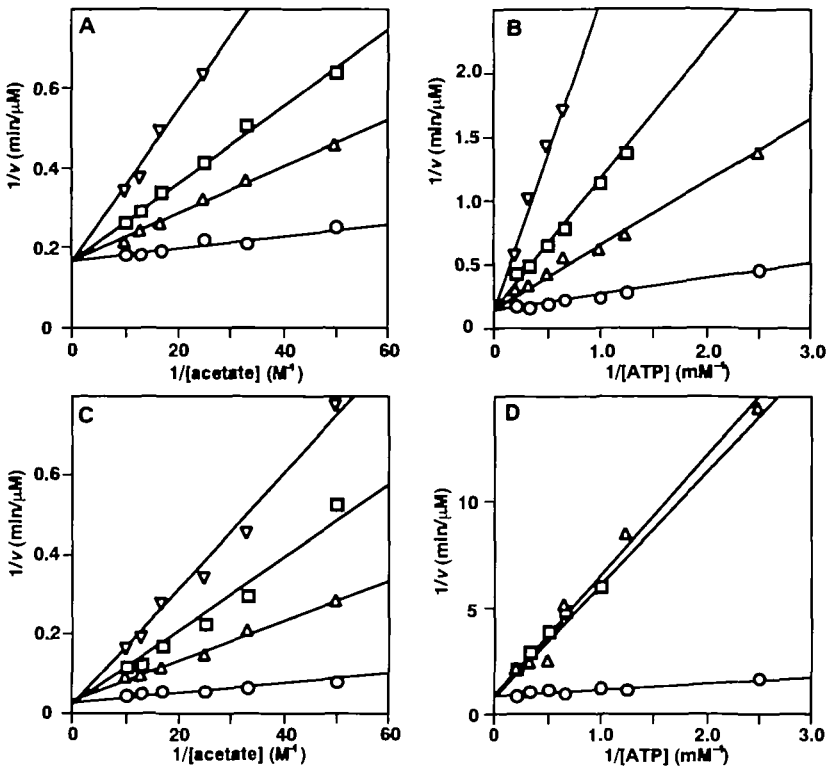

Fig. 7. **Product inhibition of AK-I and AK-II by acetyl phosphate with acetate (A, C) or ATP (B, D) as the varied substrate.** Acetyl phospate concentrations were fixed at 0 (○), 0.25 (△), 0.5 (□), and 1.0 (▽) mM. A and C: The concentrations of ATP and $MgCl_2$ were fixed to 1.0 and 5.0 mM, respectively. B and D: The concentrations of acetate and $MgCl_2$ were fixed at 30 and 5.0 mM, respectively.

TABLE III. **Comparison of kinetic constants for the forward reaction between AK-I and AK-II.**

Enzyme	Acetate		ATP		$k_{cat,F}$ (s^{-1})
	K_{ia} (mM)	K_A (mM)	K_{ib} (mM)	K_B (mM)	
AK-I	11.4	30.6	0.804	2.15	362
AK-II	17.8	26.9	2.25	3.40	310

TABLE IV. **Comparison of kinetic constants for the reverse reaction between AK-I and AK-II.**

Enzyme	Acetyl phosphate		ADP		$k_{cat,R}$ (s^{-1})
	K_{ip} (mM)	K_P (mM)	K_{iq} (mM)	K_Q (mM)	
AK-I	0.481	0.834	0.726	1.26	659
AK-II	0.332	0.758	0.774	1.77	353

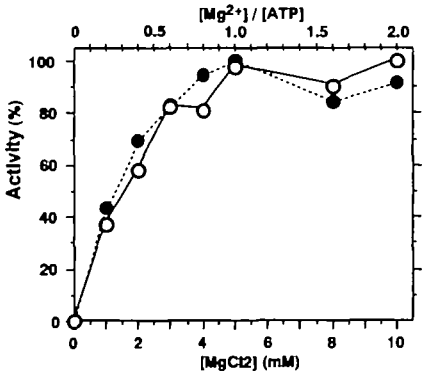

Fig. 8. **Effect of the Mg^{2+} concentration on the activity of AK-I and AK-II.** Acetate kinase activity was determined at 25°C in 50 mM HEPES (pH 7.5), 50 mM NaCl. The reaction mixture (0.1 ml) contained 5.0 mM ATP, 0.1 M acetate, and the indicated concentrations of $MgCl_2$ (0–10 mM). The total concentrations AK-I and AK-II were 4.54 and 10.5 nM , respectively. After a 9-min incubation, the reaction was stopped by the addition of 0.1 ml of 0.5 M potassium phosphate (pH 3.0). The enzymatically formed ADP was assayed by HPLC using 5 nmol of FAD as an internal standard. Open circles, AK-I; closed circles, AK-II.

unit is produced by post-tranlational chemical modification of α^S subunit, and that α^L subunit migrates abnormally on SDS-PAGE due to the modification, although the possibility remains that α^S subunit is a C-terminally truncated product of α^L subunit.

The acetate kinase gene is present in only one copy per genome of *Methanosarcina thermophila* (*17*) and *Corynebacterium glutamicum* (*11*). A single acetate kinase activity has been found in the crude extracts from a number of bacteria (*20–23, 25–29*). Two distinct forms of acetate kinase have been demonstrated only for a spirochete (*24*) and *D. vulgaris* (the present work). The two acetate kinase isozymes from the spirochete were only partially purified and no comparison was done of their peptide sequences. Interestingly, the relative amount of the two spirochete isozymes varied greatly among cells grown in different batches. Taken together, these findings strongly suggest that the two forms of acetate kinase in *D. vulgaris* are products of a single gene, and that the primary gene product is changed into distinct forms by post-translational modification depending on growth conditions.

Nitrogenase from *Rhodospirillum rubrum* is inactivated by ADP-ribosylation, and the modified enzyme shows a 31.5-kDa subunit in addition to a 30.0-kDa subunit on SDS-PAGE, while the unmodified enzyme has only 30.0-kDa subunits (*47, 48*). Like in *R. rubrum*, some post-translational modification mechanism in *D. vulgaris* may play an important role in regulation of enzymes in the bacteria.

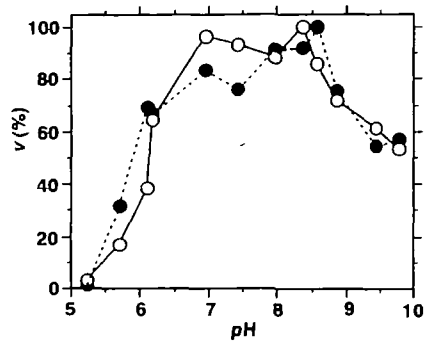

Fig. 9. **Effect of pH on the activity of AK-I and AK-II.** Acetate kinase activity was determined at 25°C in the following buffers: MES (pH 5.0–6.2), HEPES (pH 6.0–7.5), Tris (pH 7.4–8.6), and glycine (pH 8.8–10). The buffer concentration was 50 mM and all buffers contained 50 mM NaCl. The pH values of each reaction mixture were confirmed with a pH meter. The reaction mixture (0.1 ml) contained 5.0 mM ATP, 5 mM $MgCl_2$, and 0.1 M acetate. The total concentrations of AK-I and AK-II were 4.65 and 10.5 nM, respectively. Open circles, AK-I; closed circles, AK-II.

Further investigations are in progress to elucidate the difference between α^S and α^L subunits.

AK-I and AK-II showed the same requirement of Mg^{2+}, and excess Mg^{2+} did not inhibit either enzyme activity. Because the optimal Mg^{2+}/ATP ratio of 1:1 means that the actual substrate of acetate kinase is the Mg-ATP complex, the results indicate that both α^S and α^L subunits have no allosteric Mg^{2+} binding sites which affect the activity. To minimize possible systematic errors due to insufficient levels of Mg^{2+}, the present kinetic data were obtained under the condition that the ratio of Mg^{2+}/ATP or Mg^{2+}/ADP in all assay mixtures was higher than 1 (the Mg^{2+} concentration was maximally 10 mM).

The pH curves of AK-I and AK-II had a near plateau region around pH 7.5. Because both enzyme activities were least sensitive to a pH change around this pH value, kinetic experiments were done at pH 7.5 to avoid possible disturbance of pH by relatively high concentrations of substrates. As summarized in Tables III and IV, AK-I showed moderately larger turnover number than AK-II in both the forward and reverse reactions. No large difference was found in the values of dissociation constants between AK-I and AK-II except for those of K_{ib}. The K_{ib} value for AK-I is less than half of that for AK-II. This means that AK-I has 2.8-fold higher affinity to ATP than AK-II.

The present initial velocity data were well fitted to a sequential Bi Bi mechanism (*39*). As shown in Fig. 5, all double-reciprocal plots intersected within experimental errors to the left of the $1/v$ axis. A Ping Pong mechanism (*39*) could be ruled out for both AK-I and AK-II, because double-reciprocal plots did not give parallel lines. As shown in Fig. 7, acetyl phosphate inhibited competitively both acetate and ATP, supporting a rapid equilibrium random sequential Bi Bi mechanism.

The ratio of K_A and K_{ia} values (= that of K_B and K_{ib} values, Eq. 6) were 2.7 for AK-I and 1.5 for AK-II (Table III). This means that occupancy of the acetate-binding site does not strongly affect the binding of ATP to the nucleotide-binding site in the active site, and *vice versa*. This conclusion is consistent with a random model. In the reverse reaction, the ratio of K_p and K_{ip} values (= that of K_Q and K_{iq} values, Eq. 7) was 1.7 for AK-I and 2.3 for AK-II. The results indicate that the occupancy of the binding site for acetyl phosphate or ADP moderately weakens mutual binding but does not prevent binding of the other substrate. This conclusion is also consistent with a random model.

The catalytic mechanism of acetate kinase is still poorly understood. Recent progress in X-ray crystallographic study and site-directed mutagenesis study on acetate kinase from *M. thermophila* (*30*, *45*, *46*) has shed new light on the mechanism of phosphoryl transfer and on the structural basis of difference in kinetic properties among acetate kinases. Thorough kinetic studies of acetate kinase are important to address these problems, and the method developed in the present study is suitable for such studies. Molecular cloning and hyperexpression of the acetate kinase gene from *D. vulgaris* are in progress in our laboratory to understand how two forms of acetate kinase are produced and what physiological roles the enzymes play.

REFERENCES

1. Rosencrantz, D., Rainey, F.A., and Janssen, P.H. (1999) Culturable populations of *Sporomusa* spp. and *Desulfovibrio* spp. in the anoxic bulk soil of flooded rice microcosms. *Appl. Environ. Microbiol.* **65**, 3526–3533
2. Cottrell, M.T. and Cary, S.C. (1999) Diversity of dissimilatory bisulfite reductase genes of bacteria associated with the deep-sea hydrothermal vent polychaete annelid *Alvinella pompejana*. *Appl. Environ. Microbiol.* **65**, 1127–1132
3. Quattara, A.S., Patel, B.K.C., Cayol, J.-L., Cuzin, N., Traore, A.S., and Garcia, J.-L. (1999) Isolation and characterization of *Desulfovibrio burkinensis* sp. nov. from an African ricefield, and phylogeny of *Desulfovibrio alcoholivorans*. *Int. J. Syst. Bacteriol.* **49**, 639–643
4. Okabe, S., Itoh, T., Satoh, H., and Watanabe, Y. (1999) Analyses of spatial distributions of sulfate-reducing bacteria and their activity in aerobic wastewater biofilms. *Appl. Environ. Microbiol.* **65**, 5107–5116
5. van Schie, P.M. and Fletcher, M. (1999) Adhesion of biodegradative anaerobic bacteria to solid surfaces. *Appl. Environ. Microbiol.* **65**, 5082–5088
6. Nielsen, J.T., Liesack, W., and Finster, K. (1999) *Desulfovibrio zosterae* sp. nov., a new sulfate reducer isolated from surface-sterilized roots of the seagrass *Zostera marina*. *Int. J. Syst. Bacteriol.* **49**, 859–865
7. Fröhlich, J., Sass, H., Babenzien, H.-D., Kuhnigk, T., Varma, A., Saxena, S., Nalepa, C., Pfeiffer, P., and König, H. (1999) Isolation of *Desulfovibrio intestinalis* sp. nov. from the hindgut of the lower termite *Mastotermes darwiniensis*. *Can. J. Microbiol.* **45**, 145–152
8. Boyle, A.W., Phelps, C.D., and Young, L.Y. (1999) Isolation from estuarine sediments of a *Desulfovibrio* strain which can grow on lactate coupled to the reductive dehalogenation of 2,4,6-tribromophenol. *Appl. Environ. Microbiol.* **65**, 1133–1140
9. Akutsu, H., Park, J.-S., and Sano, S. (1993) L-Methionine methyl is specifically incorporated into the C-2 and C-7 positions of the porphyrin of cytochrome c_3 in a strictly anaerobic bacterium, *Desulfovibrio vulgaris*. *J. Am. Chem. Soc.* **115**, 12185–12186
10. Ishida, T., Yu. L., Akutsu, H., Ozawa, K., Kawanishi, S., Seto, A., Inubushi, T., and Sano, S. (1998) A primitive pathway of porphyrin biosynthesis and enzymology in *Desulfovibrio vulgaris*. *Proc. Natl. Acad. Sci. USA* **95**, 4853–4858
11. Reinscheid, D.J., Schnicke, S., Rittmann, D., Zahnow, U., Sahm, H., and Eikmanns, B.J. (1999) Cloning, sequence analysis, expression and inactivation of the *Corynebacterium glutamicum pta-ack* operon encoding phosphotransacetylase and acetate kinase. *Microbiology* **145**, 503–513

12. Dailey, F.E. and Berg, H.C. (1993) Change in direction of flagellar rotation in *Escherichia coli* mediated by acetate kinase. *J. Bacteriol.* **175**, 3236–3239
13. Prüß, B.M. and Wolfe, A.J. (1994) Regulation of acetyl phosphate synthesis and degradation, and the control of flagellar expression in *Escherichia coli*. *Mol. Microbiol.* **12**, 973–984
14. Liu, C-L. and Peck, H.D., Jr. (1981) Comparative bioenergetics of sulfate reduction in *Desulfovibrio* and *Desulfotomaculum* spp. *J. Bacteiol.* **145**; 966–973
15. Brown, M.S. and Akagi, J.M. (1966) Purification of acetokinase from *Desulfovibrio desulfuricans*. *J. Bacteriol* **92**, 1273–1274
16. Matsuyama, A., Yamamoto, H., and Nakano, E. (1989) Cloning, expression, and nucleotide sequence of the *Escherichia coli* K-12 *ackA* gene. *J. Bacteriol.* **171**, 577–580
17. Latimer, M.T. and Ferry, J.G. (1993) Cloning, sequence analysis, and hyperexpression of the genes encoding phosphotransacetylase and acetate kinase from *Methanosarcina thermophila*. *J. Bacteriol.* **175**, 6822–6829
18. Boynton, Z.L., Bennett, G.N., and Rudolph, F.B. (1996) Cloning, sequencing, and expression of genes encoding phosphotransferase and acetate kinase from *Clostridium acetobutylicum* ATCC 824. *Appl. Environ. Microbiol.* **62**, 2758–2766
19. Summers, M.L., Denton, M.C., and McDermott, T.R. (1999) Genes coding for phosphotransacetylase and acetate kinase in *Sinorhizobium meliloti* are in an operon that is inducible by phosphate stress and controlled by PhoB. *J. Bacteriol.* **181**, 2217–2224
20. Nakajima, H., Suzuki, K., and Imahori, K. (1978) Purification and properties of acetate kinase from *Bacillus stearothermophilus*. *J. Biochem.* **84**, 193–203
21. Yoshimura, F. (1978) Purification and characterization of acetate kinase from *Veillonella alcalescens* ATCC 17748. *Arch. Biochem. Biophys.* **189**, 424–432
22. Griffith, M.J. and Nishimura, J.S. (1979) Acetate kinase from *Veillonella alcalescens*: Purification and physical properties. *J. Biol. Chem.* **254**, 442–446
23. Kahane, I. and Muhlrad, A. (1979) Purification and properties of acetate kinase from *Acholeplasma laidlawii*. *J. Bacteriol.* **137**, 764–772
24. Harwood, C.S. and Canale-Parola, E. (1982) Properties of acetate kinase isozymes and a branched-chain fatty acid kinase from a spirochete. *J. Bacteriol.* **152**, 246–254
25. Fox, D.K. and Roseman, S. (1986) Isolation and characterization of homogeneous acetate kinase from *Salmonella typhimurium* and *Escherichia coli*. *J. Biol. Chem.* **261**, 13487–13497
26. Aceti, D.J. and Ferry, J.G. (1988) Purification and characterization of acetate kinase from acetate-grown *Methanosarcina thermophila*: Evidence for regulation of synthesis. *J. Biol. Chem.* **263**, 15444–15448
27. Diez-Gonzalez, F., Russell, J.B., and Hunter, J.B. (1997) The acetate kinase of *Clostridum acetobutylicum* strain P262. *Arch. Microbiol.* **166**, 418–420
28. Winzer, K., Lorenz, K., and Dürre, P. (1997) Acetate kinase from *Clostridium acetobutylicum*: a highly specific enzyme that is actively transcribed during acidogenesis and solventgenesis. *Microbiology* **143**, 3279–3286
29. Bock, A.-K., Glasemacher, J., Schmidt, R., and Schönheit, P. (1999) Purification and characterization of two extremely thermostable enzymes, phosphate acetyltransferase and acetate kinase, from the hyperthermophiliceubacterium *Thermotoga maritima*. *J. Bacteriol.* **181**, 1861–1867
30. Buss, K.A., Ingram-Smith, C., Ferry, J.G., Sanders, D.A., and Hasson, M.S. (1997) Crystallization of acetate kinase from *Methanosarcina thermophulla* and prediction of its fold. *Protein Sci.* **6**, 2659–2662
31. Postgate, J.R. (1984) *Sulfate-Reducing Bacteria*, 2nd ed., Cambridge Univeysity Press, Cambridge, U.K.
32. Nishimura, J.S. and Griffith, M.J. (1981) Acetate kinase from *Veillonella alcalescens* in *Methods in Enzymology* (Lowenstein, J.M., ed.) Vol. 71, pp. 311–316, Academic Press, New York
33. Laemmli, U.K. (1970) Cleavage of structural proteins during the assembly of the head of bacteriophage T4. *Nature* **227**, 680–685
34. Hayashi, Y., Matsui, H., and Takagi, T. (1989) Membrane protein molecular weight determined by low-angle laser light scattering photometry coupled with high-performance gel chromatography in *Methods in Enzymology* (Fleischer, S. and Fleischer, B., eds.) Vol. 172, pp. 514–528, Academic Press, San Diego
35. Ishida, T., Narita, M., Nozaki, M., and Horiike, K. (1996) Selective cleavage and modification of the intersubunit disulfide bonds of bovine dopamine β-monooxygenase: Conversion of tetramer to active dimer. *J. Biochem.* **120**, 346–352
36. Kobayashi, T., Ishida, T., Horiike, K., Takahara, Y., Numao, N., Nakazawa, A., Nakazawa, T., and Nozaki, M. (1995) Overexpression of *Pseudomonas putida* catechol 2,3-dioxygenase with high specific activity by genetically engineered *Escherichia coli*. *J. Biochem.* **117**, 614–622
37. Blättler, W.A. and Knowles, J.R. (1979) Stereochemical course of phosphokinases. The use of adenosine [γ-(S)-^{16}O,^{17}O,^{18}O]triphosphate and the mechanistic consequences for the reactions catalyzed by glycerol kinase, hexokinase, pyruvate kinae, and acetate kinase. *Biochemistry* **18**, 3927–3933
38. Spector, L.B. (1980) Acetate kinase: A triple-displacement enzyme. *Proc. Natl. Acad. Sci. USA* **77**, 2626–2630
39. Cleland, W.W. (1963) The kinetics of enzyme-catalyzed reactions with two or more substrates or products: I. nomenclature and rate equations. *Biochim. Biophys. Acta* **67**, 104–137
40. Purich, D.L. and Fromm, H.J. (1972) Evaluation of the phosphoryl-enzyme intermediate concept in the acetate kinase and hexokinase reactions from kinetic studies. *Arch. Biochem. Biophys.* **149**, 307–315
41. Todhunter, J.A. and Purich, D.L. (1974) Evidence for the formation of a γ-phosphorylated glutamyl residue in the *Escherichia coli* acetate kinase reaction. *Biochem. Biophys. Res. Commun.* **60**, 273–280
42. Janson, C.A. and Cleland, W.W. (1974) The inhibition of acetate, pyruvate, and 3-phosphoglycerate kinases by chromium adenosine tirphosphate. *J. Biol. Chem.* **249**, 2567–2571
43. Wong, S.S. and Wong. L.-J.C. (1980) Inactivation of *Escherichia coli* acetate kinase by N-ethylmaleimide: Protection by substrates and products. *Biochim. Biophys. Acta* **615**, 121–131
44. Wong, S.S. and Wong. L.-J.C. (1981) Evidence for an essential arginine residue at the active site of *Escherichia coli* acetate kinase. *Biochim. Biophys. Acta* **660**, 142–147
45. Singh-Wissmann, K., Ingram-Smith, C., Miles, R.D., and Ferry, J.G. (1998) Identification of essential glutamates in the acetate kinase from *Methanosarcina thermophila*. *J. Bacteriol.* **180**, 1129–1134
46. Singh-Wissmann, K., Miles, R.D., Ingram-Smith, C., and Ferry, J.G. (2000) Identification of essential arginines in the acetate kinase from *Methanosarcina thermophila*. *Biochemistry* **39**, 3671–3677
47. Gotto, J.W. and Yoch, D.C. (1982) Regulation of *Rhodospirillum rubrum* nitrogenase activity: Properties and interconversion of active and inactive Fe protein. *J. Biol. Chem* **257**, 2868–2873
48. Durner, J., Böhm, I., Hilz, H., and Böger, P. (1994) Posttranlational modification of nitrogenase: Differences between the purple bacterium *Rhodospillum rubrum* amd the cyanobacterium *Anabaena variabilis*. *Eur. J. Biochem* **220**, 125–130